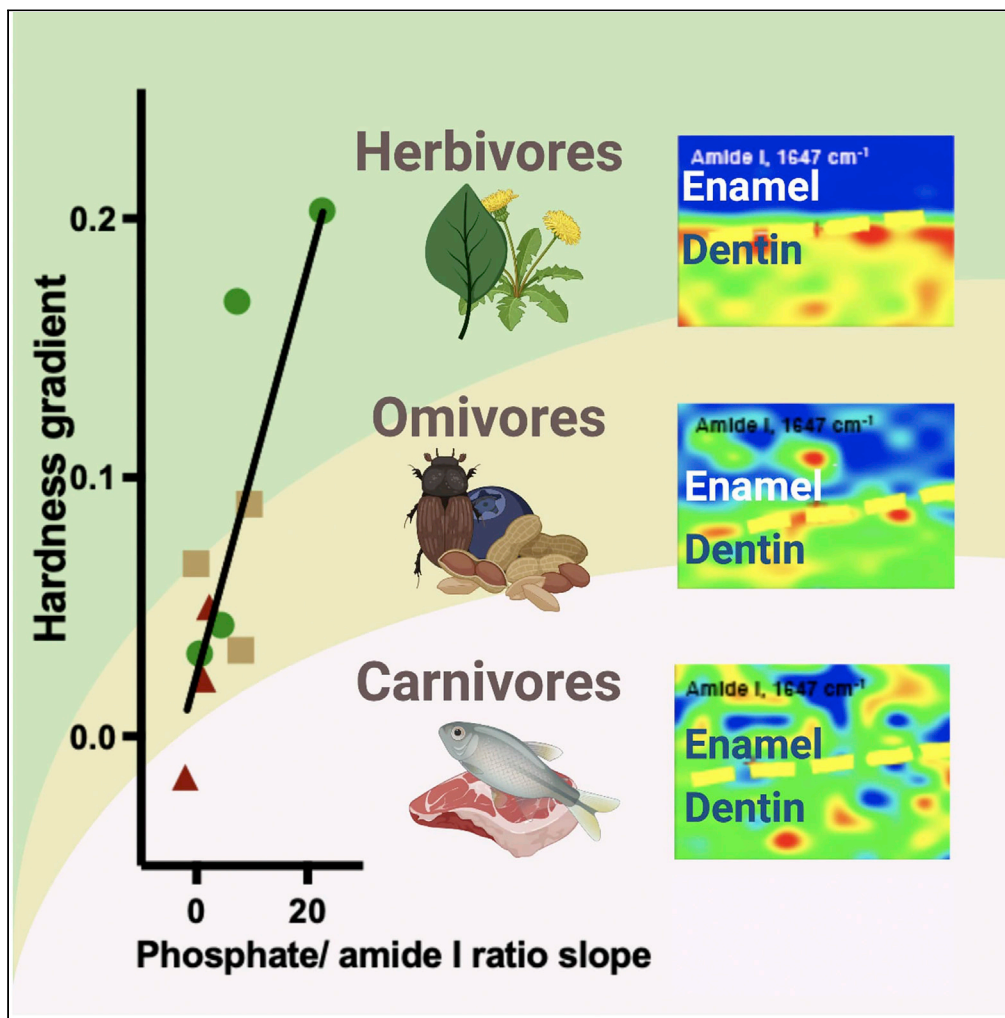


Article

Mammalian tooth enamel functional sophistication demonstrated by combined nanotribology and synchrotron radiation FTIR analyses



Chen-Tzu Chiu,
Jyun-Kai Cao, Pei-
Wen Wang, ...,
Yeau-Ren Jeng,
Dar-Bin Shieh,
Robert R. Reisz

imeyrj@gs.ncku.edu.tw (Y.-
R.J.)
dbsieh@mail.ncku.edu.tw
(D.-B.S.)
robert.reisz@utoronto.ca
(R.R.R.)

Highlights

Diet drives the evolution
of enamel composition
and adaptive mechanical
properties

Herbivores tend to have
the highest enamel
surface hardness

Evolutionary changes
enable enamel hardness
gradient profiles for diet
and longevity

Enamel hardness gradient
corresponds to the in situ
phosphate-to-amide ratio

Chiu et al., iScience 26,
105679
January 20, 2023 © 2022
[https://doi.org/10.1016/
j.isci.2022.105679](https://doi.org/10.1016/j.isci.2022.105679)



Article

Mammalian tooth enamel functional sophistication demonstrated by combined nanotribology and synchrotron radiation FTIR analyses

Chen-Tzu Chiu,^{1,14} Jyun-Kai Cao,^{2,14} Pei-Wen Wang,^{1,3} Ya-Na Wu,^{1,4} Yao-Chang Lee,^{5,6,7} Yeau-Ren Jeng,^{2,8,9,10,*} Dar-Bin Shieh,^{1,3,4,11,*} and Robert R. Reisz^{12,13,15,*}

SUMMARY

The teeth of limbed vertebrates used for capturing and processing food are composed of mineralized dentine covered by hypermineralized enamel, the hardest material organisms produce. Here, we combine scanning probe microscopy, depth sensing, and spectromicroscopy (SR-FTIR) to characterize the surface ultrastructural topography, nanotribology, and chemical compositions of mammal species with different dietary habits, including omnivorous humans. Our synergistic approach shows that enamel with greater surface hardness or thickness exhibited a more salient gradient feature from the tooth surface to the dentino-enamel junction (DEJ) one that corresponds to the *in situ* phosphate-to-amide ratio. This gradient feature of enamel covering softer dentine is the determining factor of the amazingly robust physical property of this unique biomaterial. It provides the ability to dissipate stress under loading and prevent mechanical failure. Evolutionary change in the biochemical composition and biomechanical properties of mammalian dentition is related to variations in the oral processing of different food materials.

INTRODUCTION

Tooth enamel possesses unique physical mechanical properties with intricate structure at the micro-nano-scale and hierarchical organization. It is fascinating how enamel with both brittle (mineral) and soft (protein) components could be integrated to exhibit properties of both rigidity and resistance to mechanical failure. This has led scientists to explore abiotic columnar nanocomposites to mimic tooth enamel for high-performance load-bearing materials.¹ Mineralized tissues are critical features in vertebrate evolution. They include protective body armor, an endoskeleton for locomotion, and teeth for feeding, the latter being a key innovation fundamental to much of vertebrate success. Among these tissues, the evolution of hypermineralized enamel in vertebrate teeth represents a significant innovation, allowing various stem tetrapods and their descendants to acquire energy from a great variety of other organisms through multiple methods of oral processing. As exemplified by mammals, oral mechanical trituration appears to have been an essential evolutionary sophistication in feeding behavior.² Dentition is also the most abundant resource in the fossil record through geologic time due to its extremely high mineral content.^{3,4} Teeth often retain nanoscopic characteristics through geologic time, allowing comprehensive investigation of the evolutionary sophistication from structural and trace chemical evidence at a different hierarchical scale.

Initially, teeth were mainly composed of naked dentine, as in *Psarolepis romeri*, about 400 Mya. Although enamel-like material was already present in the scales of ancient fishes for protection,^{5–8} the evolution of true enamel on teeth was gradual. Vertebrate teeth evolved an enamel covering through a broad spectrum of intermediate structures. True enamel began to be present only in Devonian stem tetrapods and is characterized by amelogenin-dominant protein matrix secreted by ameloblasts of epithelial origin.⁹ Amelogenin is known to degrade as the tooth matures to fully hypermineralized tissues gradually. In most tetrapods, including amphibians and reptiles, these enamels formed semi-parallel crystallites of hydroxyapatite that radiate outward from the dentinal-enamel junction (DEJ). The DEJ unites the brittle overlying thin enamel with the relatively softer and more elastic dentin to form the bulk of the tooth crown. In addition, such structural integration appears to confer excellent toughness and crack-deflecting properties and has drawn considerable interest as a biomimetic model for uniting dissimilar materials to gain optimal mechanical

¹School of Dentistry and Institute of Oral Medicine, National Cheng Kung University, Tainan 701401, Taiwan

²Department of Mechanical Engineering, National Chung Cheng University, Chia-Yi 62100, Taiwan

³Center of Applied Nanomedicine and Core Facility Center, National Cheng Kung University, Tainan 701401, Taiwan

⁴iMANI Center of the National Core Facility for Biopharmaceuticals, National Science and Technology Council, Taipei 106214, Taiwan

⁵Life Science Group, National Synchrotron Radiation Center, Hsinchu 30076, Taiwan

⁶Department of Optics and Photonics, National Central University, Chung-Li 32001, Taiwan

⁷Department of Chemistry, National Tsing Hua University, Hsinchu 30013, Taiwan

⁸Department of Biomedical Engineering, National Cheng Kung University, Tainan 70101, Taiwan

⁹Medical Device Innovation Center, National Cheng Kung University, Tainan 70101, Taiwan

¹⁰Academy of Innovative Semiconductor and Sustainable Manufacturing, National Cheng Kung University, Tainan 70101, Taiwan

¹¹Department of Stomatology, National Cheng Kung University Hospital, Tainan 704302, Taiwan

¹²International Centre of Future Science, Dinosaur Evolution Research Center,

Continued



functions.^{10,11} On the other side of tetrapod evolution, mammals and their fossil predecessors gradually evolved thicker enamel and refined cylindrical or hemicylindrical enamel prisms bundled into parallel crystallites in designed topological substructures. These enamel prisms achieved advanced anisotropic properties, especially in higher mammals where more proteins are involved in shaping functional sophistication.

Human dentition has been extensively studied. It was previously discovered that nanohardness and the elastic modulus have a specific spatial distribution in the enamel rods in human molariform teeth with a built-in gradient between the external enamel surface and the DEJ.^{12,13} Such variation in the form of a gradient correlates well with the decreasing trend of calcium composition from *in situ* element analysis. There is a clear advantage of such a gradient design, promoting resistance to penetration, energy dissipation, and mitigation of fracture, all critical for the performance of human teeth^{14,15} and other mineralized biomaterials.¹¹ The nature of tooth enamel microstructure ranging from dinosaurs to humans has also been previously documented¹⁶⁻¹⁸, but no comprehensive analysis comparing different species of mammals with other diets has been undertaken. Hence, there has been no clear understanding of the evolution of enamel as it relates to a diet of mammals, the large clade that includes humans.

Given our comparative study using a diversity of mammalian dentition, our novel study incorporating teeth from various species of related taxa provides new insights into the evolution of the well-known characteristics of human dentition. In this study, we collected teeth from 11 different mammal species and a non-mammalian amniote as a representative of the outgroup. We analyzed their nano-tribological properties with *in situ* profiling of synchrotron radiation Fourier transform infrared spectroscopy (SR-FTIR) spectra signature and detailed anatomical structures to understand better their intriguing properties and how they conformed to the evolution of their feeding behaviors.

RESULTS

Surface hardness and the tribological profile in the longitudinal section of tooth enamel

We characterized two types of hardness of the tooth enamel, one on the surface of enamel denoted by surface hardness and the other along the longitudinal section of enamel from the top surface to the DEJ, indicated as longitudinal hardness. The hardness gradient is the slope of the longitudinal hardness from the top surface to the dentino-enamel junction. Investigations of the functional hardness gradient characteristics and prism arrangements of the tooth enamel in different species indicate that two key factors contribute to the remarkable mechanical properties of the enamel. The hardness of enamel measured by nanoindentation showed that the hardness values mainly ranged between 3 and 6 GPa. A significant trend of higher surface hardness was observed among herbivores followed by omnivores and carnivores (Figure 1A), and the mean surface hardness of the enamel in herbivores (p value <0.05) and omnivores was significantly higher than in carnivores (Figure 1B). However, this trend was not explicitly presented in the hardness gradient (Figures 1C and 1D).

The surface hardness of the enamel in different species appears closely related to their feeding habits. Herbivores tend to have the highest surface hardness, whereas carnivores have much lower values. The hardness gradient between the outer surface and the inner structure shows intriguing features, with higher surface hardness displaying a more significant hardness gradient, especially among herbivores. Herbivores (Figure 2A) and omnivores (Figure 2B) possess greater thickness and hardness gradient of enamel than carnivores (Figure 2C). Our study, therefore, provides evidence to support the existence of significant variation in the tribological gradient in the enamels of various mammal species. In addition, the thickness of enamel and hardness distribution patterns of teeth were calculated to analyze the correlation. Our results show a significant ($p < 0.01$) correlation between hardness gradient and thickness of enamel among all collected species (Figure 2D).

A previous study¹⁹ showed that the fulcrum points of the mastication system of herbivores and omnivores are at much higher positions than that of the carnivores, so the upper and lower jaws are presented in a loose jaw attachment, which allows herbivores and omnivores to exert grinding movements. Reports also show that enamel microstructure plays a critical role in the mechanisms of damage resistance and the adaptation to their diet.²⁰ Canines and carnassials (molars with cutting function) teeth of carnivores must rely on the jaw's up and down movement to puncture and cut food. Thus, carnivores form a lock jaw attachment, which enables the upper and lower jaws to slide vigorously and drive the upper and lower cutting and tearing motion of the canine and the molars, and the temporalis muscle is dominant. In

Jilin University, Changchun,
Jilin 130012, China

¹³Department of Biology,
University of Toronto
Mississauga, Mississauga,
ON, Canada

¹⁴These authors contributed
equally

¹⁵Lead contact

*Correspondence:
imeyrj@gs.ncku.edu.tw
(Y.-R.J.),
dbshieh@mail.ncku.edu.tw
(D.-B.S.),
robert.reisz@utoronto.ca
(R.R.R.)

<https://doi.org/10.1016/j.isci.2022.105679>

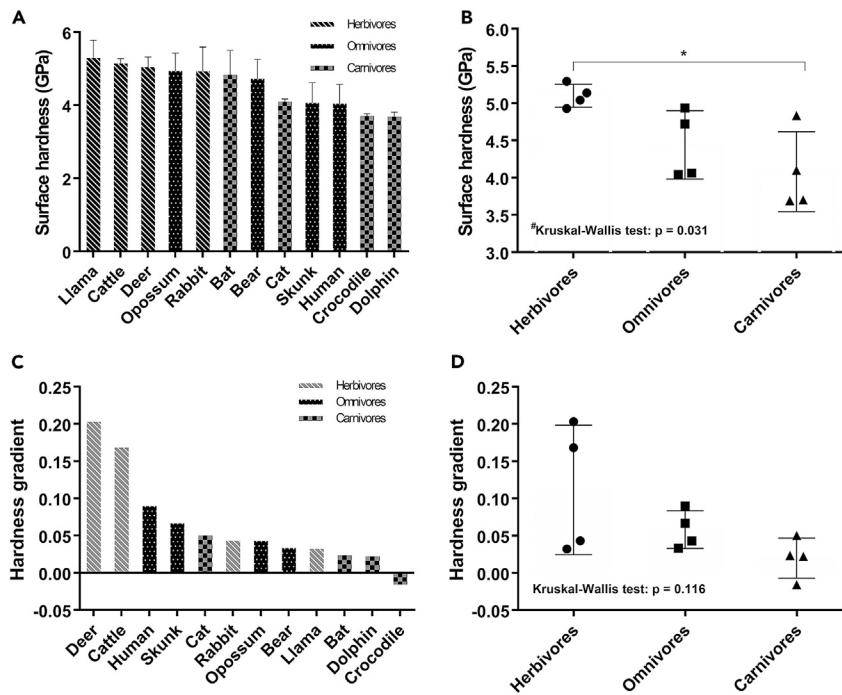


Figure 1. Surface hardness of the tooth enamel on the longitudinal section

(A) The surface hardness of tooth enamel among 12 different animal species (11 mammals and one reptile). The tested samples mainly were between 3 and 6 Gpa for their enamel surfaces. Herbivores showed higher surface hardness, followed by omnivores than carnivores.

(B) Kruskal-Wallis was used to test differences between three groups and showed a significant difference between herbivores, omnivores, and carnivores. #Kruskal-Wallis test: $p = 0.031$. Wilcoxon rank sum analysis was used to conduct a post-hoc test for the correlation between the tooth surface hardness stratified by their dietary habits. The mean surface hardness of herbivores (5.101 Gpa) is higher than that of the omnivores (4.44 Gpa, $p = 0.061$) and carnivores (4.081 Gpa, $*p = 0.030$). No statistical significance was found between omnivores and carnivores ($p = 0.471$).

(C) The hardness gradient distribution across the longitudinal enamel section from the tooth surface to the dentinal-enamel junction was illustrated. Strikingly, the hardness gradient of deer and cattle values were far more significant than others.

(D) The statistical analysis of tooth enamel hardness gradient stratified by their feeding habits was presented.

contrast, the masseter is the most significant jaw-closer muscle in herbivores and omnivores, where chewing action predominates. Our experimental results indicate that the high hardness of the tooth surface may require a hardness gradient to minimize tooth wearing from grinding foods. The hardness gradient plays a significant role in the capability of a given material to absorb more energy without breaking. Our results indicate that the hardness gradient of mammalian molar teeth could contribute to their ability to withstand deformation during chewing, which is associated with the ability to absorb energy, as shown for herbivores and omnivores. On the other hand, enamel thickness appears to be related to the animals' longevity, where the greater thickness was present in the longer-living mammal, including humans.

Longevity and mechanical properties of enamel

Mammals use their teeth in oral processing, and their hardness should be closely related to their feeding behavior throughout life. Mammals retain their adult teeth throughout life (diphyodonty), unlike crocodiles and most other reptiles, where teeth are repeatedly replaced (polyphyodonty). The surface hardness of some herbivorous mammals appears not to be highly correlated with longevity (Figure 3A), partly because some herbivores evolved continuously growing teeth. The coefficient of determination showed a satisfactory correlation between hardness gradient and their longevity in herbivores and omnivores as well as carnivores (Figure 3B). And there is a similar trend in the correlation between the thickness of the enamel and their longevity in herbivores and omnivores groups (Figure 3C). In the evolution of mammals, the shape of the teeth was evolved into different forms depending on their food intake. Omnivorous mammals,

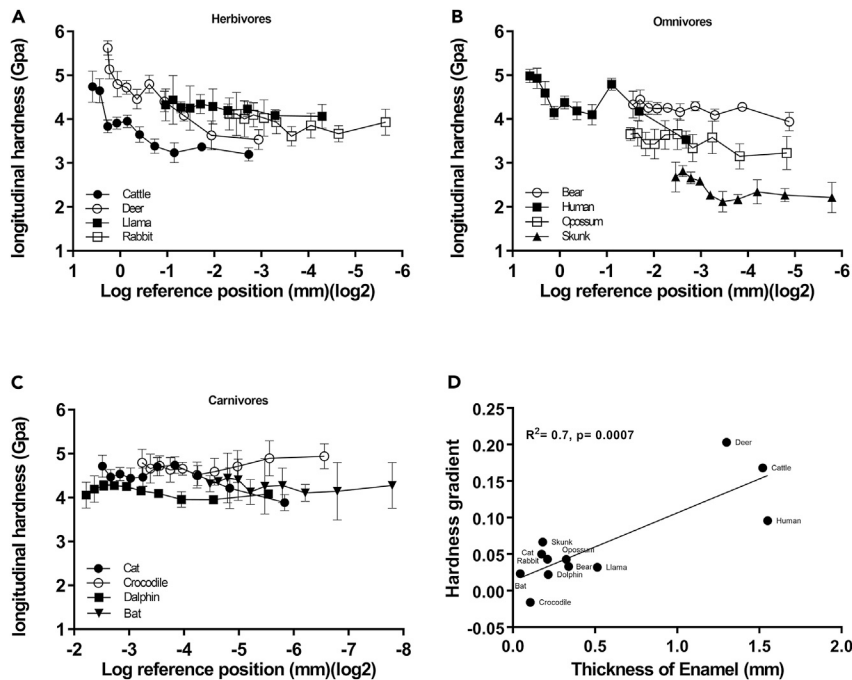


Figure 2. The correlation between enamel hardness on each reference position over the longitudinal section of the teeth

(A–C) Nanoindenter analyzed the hardness of tooth enamel from the collected species from the respective tooth surface site toward DEJ. Each reference position along the longitudinal section of (A) herbivores, (B) omnivores, and (C) carnivores was presented.

(D) Correlation between the hardness gradient from the enamel surface to DEJ versus the enamel thickness among the 12 animal species was illustrated ($R^2 = 0.7$, $p = 0.0007$).

including humans, use their molars for a combination of shearing and grinding, while herbivores emphasize grinding and carnivores emphasize shearing. Thus, herbivores often tend to have massive molars, and their enlarged, frequently quired-up occlusal surfaces are complex and aligned to facilitate grinding cellulose-rich plants, usually covered with grit. On the other hand, the molars of the carnivores tend to become elongated to facilitate shearing and cutting muscles, with the upper and lower molars aligned to cut and shear.²¹

Enamel with increasing gradient slope in hardness possesses more extraordinary energy dissipation ability. Furthermore, enamel with increasing thickness or hardness requires a higher gradient feature to prevent damage under dental trauma (see Figure S1). Our results indicate that a species demanding substantial grinding for nutrient intake would possess a higher hardness of enamel together with a higher gradient feature. This shows the ability of Mother Nature to develop a resilient property through evolutionary sophistication.

Similarly, the enamel of a species with greater longevity (and size) would have both greater thickness and a higher gradient slope. It is astonishing that evolution not merely develops similar gradient feature across different species but further enables the corresponding distinct gradient profiles according to their respective diet and longevity. The combination of our computational simulation and our experimental results indicates that the higher surface hardness of the teeth may require a more significant hardness gradient to support energy dissipation during dental occlusion. This happens in herbivores that require a longer time to grind foods with tough fibers than carnivores that mainly process relatively soft meats.

Biochemical distribution of hydroxyapatite and protein contents in the tooth

Enamel is the hardest animal tissue and contains up to 95% mineral with water and organic matrix for the rest. The primary mineral content is hydroxyapatite, a crystalline calcium phosphate. At the same time, the

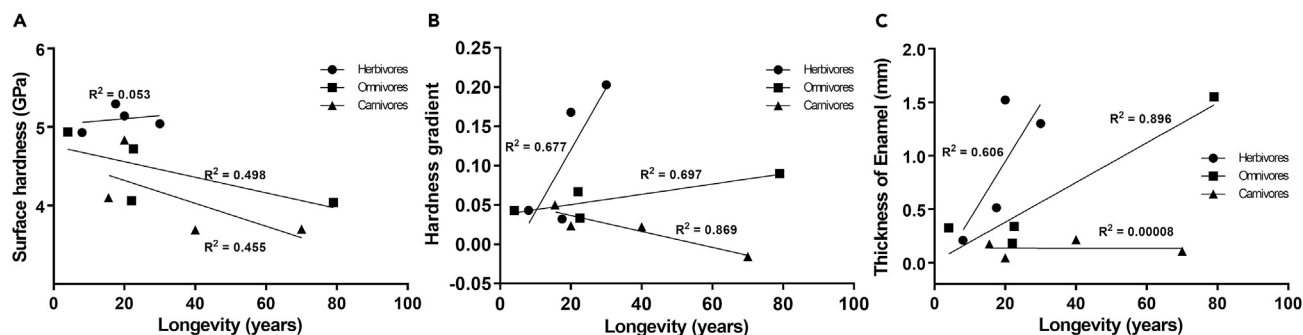


Figure 3. The correlations between enamel's mechanical properties and the species' average longevity are stratified by different feeding habits (A–C) The correlations between surface hardness, (B) hardness gradient of enamel, and (C) thickness of enamel versus the longevity of species stratified by different feeding habits. The coefficient of determination showed a satisfactory correlation between hardness gradient and longevity in herbivores, omnivores, and carnivores. A similar trend was observed in the correlation between the thickness of the enamel and its longevity among all species.

organic matrix is composed of enamel matrix proteins such as amelogenin and enamelin, as well as the type I collagen that constitutes the primary organic matrix of dentin. Infrared absorption bands at $1,647$ and $1,120\text{ cm}^{-1}$ were applied for spectroscopic mapping of the tooth cross-section using SR-FTIR microspectroscopy (Figures 4A–4C and S2). The wave number at $1,647\text{ cm}^{-1}$ represents amide I (carbonyl group, $\text{C}=\text{O}$, stretching vibration of peptide bond of protein) from proteins (amelogenin, enamelin, and collagen). The $1,120\text{ cm}^{-1}$ corresponds to the phosphate signature from the hydroxyapatite. The mapping was done in several representative areas across the dentin and the outer surface of the enamel. The results showed that the amide I (protein) to phosphate (mineral) ratios measured from dentin to enamel by SR-FTIR (in pseudocolor) has a consistent gradient with that of the respective tribological measurements. Therefore, it is conceivable that dentin has lower amide I to phosphate ratios than enamel in all species as dentin contains only about 70% mineral while enamel has over 90% inorganic contents.

Interestingly, there is a significant decline in the amide I to phosphate ratios from the outer surface of the enamel to DEJ. Such gradients of decrease in mineral content differ significantly among species. Furthermore, the gradient of mineral content decline from surface to DEJ corresponds well to the tribological measurement in the hardness gradient, suggesting the role of mineral to matrix ratio in their tribological characters.

With *in situ* nanoindentation mapping and SR-FTIR spectra signature profiling of the same tooth, we can display and compare the *in situ* endogenous biomechanical gradient and the corresponding chemical compositions (Figure 4D). The coefficient of determination showed a correlation between biomechanical gradient and chemical composition of enamels in all species. This result demonstrates that the hardness gradient of the longitudinal section is controlled by phosphate, and the gradient property is controlled by the ratio of organic to inorganic matter, which provides the teeth with good mechanical properties.

Microstructure and mechanical properties of tooth enamel

The atomic force microscopy combined with automatic image processing showed distinct prism structures among species with different feeding habits, with herbivores usually having ellipse or slender shapes. At the same time, that of the omnivores resembled a circular arc or an ellipse, with carnivores having mostly round outlines (Figure 5). The primary mineral of a tooth is hydroxyapatite, a crystalline calcium phosphate.²² At the same time, the organic matrix is composed of enamel proteins such as amelogenin and enamelin.^{23,24} The role of these proteins is believed to serve as a framework in enamel development and a supporting matrix in the adult tooth to glue the mineral contents together while providing adequate elastic modulus for the structure. Our observation displays that the prism arrangement in tooth enamel is like the architectural building blocks at the nanoscale or as a nanocomposite in the bulk state. It incorporates atomic or molecular design into an advanced nanostructure that displays distinct mechanical, chemical, and biological properties to support the evolutionary sophistication of the feeding system. Such a concept could also be applied to the fabrication and assembly of new artificial materials, giving them extraordinary flexibility and improved physical properties. In general, the

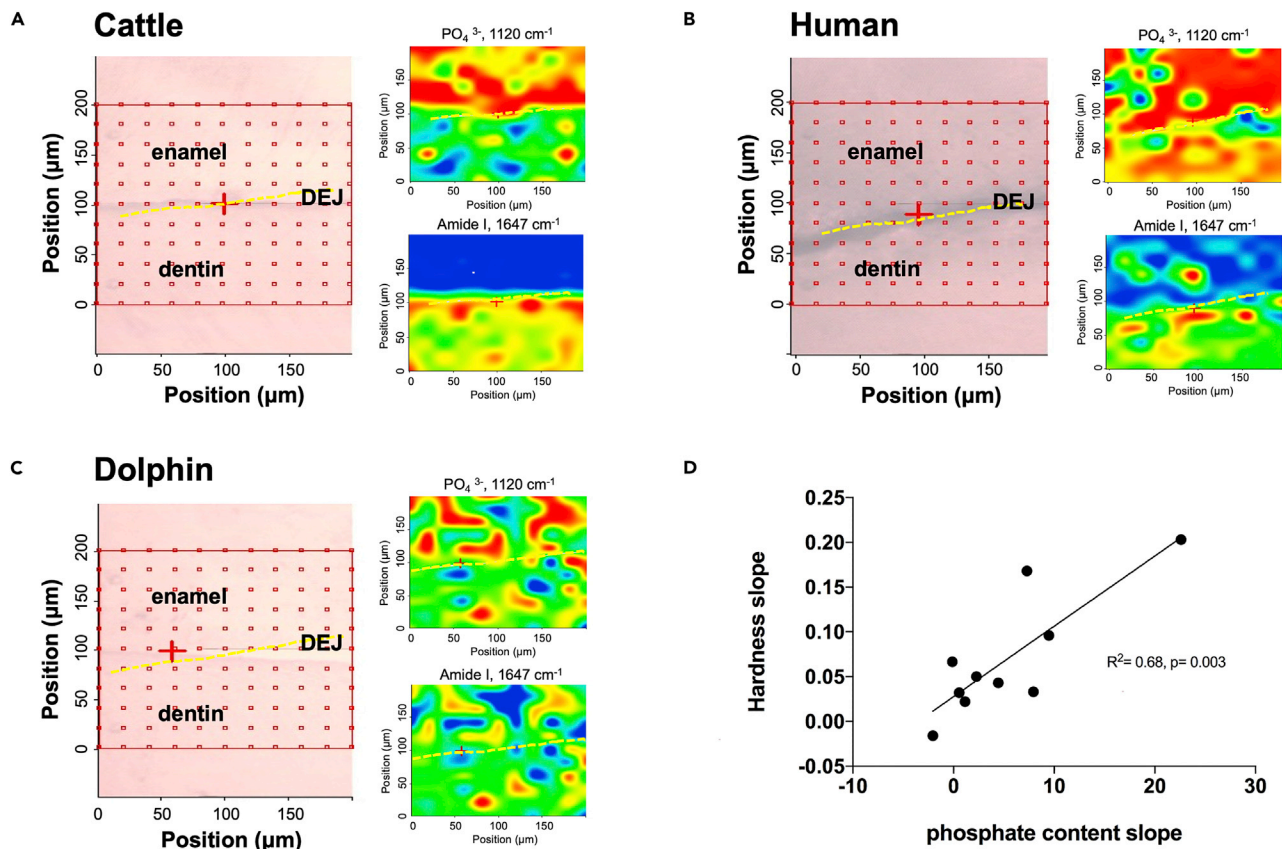


Figure 4. Correlation between enamel hardness gradient and the phosphate to matrix ratio of the tooth in various species of different feeding habits

(A–C) Representative pseudo-colored images from *in situ* profiling SR-FTIR spectra signature in teeth of varying animal species. The optical microscopy images of the prepared tooth sample cross-section from the outer enamel surface (upper) to dentin (lower) were shown in the left panel with DEJ labeled as a yellow dot line. Infrared absorption bands of the same area were mapped at $1,647\text{ cm}^{-1}$ (upper right panel) and $1,120\text{ cm}^{-1}$ (lower right panel) by SR-FTIR microspectroscopy to present the area contents of protein and apatite.

(D) The biomechanical gradient was correlated with the chemical composition of enamels ($\text{PO}_4/\text{Amide I}$ ratio) among all species. The hardness gradient in the longitudinal section was mainly attributed to the phosphate content from the hydroxyapatite of the tooth.

nanoreinforcement is dispersed into the matrix during enamel formation by the Tomes' process of ameloblasts.²⁵ The percentage by weight (mass fraction) of the mineral nanoparticles introduced into the composite system can be minimal (on the order of 0.5%–5%) yet significantly impact their property improvement due to the low filler percolation threshold.²⁶ The corresponding matrix proteins in the enamel rods may play a role, like reinforcing steel bars in the cement, while the hydroxyapatite crystals are like stone fillers. The combination of these elements delivered unprecedented hardness and elasticity to the teeth, allowing them to dissipate stresses when subjected to external forces. The tooth structure undergoing such dedicated evolution is an excellent artwork from nature. An astonishing similarity in biomechanical properties of tooth enamel was observed among all 12 species with different feeding habits. Such design can be the blueprint for developing the next generation of advanced materials.

Further study has demonstrated that the outer enamel has a limited energy dissipation potential through inelastic deformation, indicating that the outer enamel has a low ability to resist fracture. In contrast, enamel close to DEJ has a much higher capacity to dissipate energy than outer enamel. In addition, the endogenous mechanical property gradients in the human enamel significantly improved the resistance to fracture penetration and energy dissipation to provide long-term use of the dentition, critical for obtaining nutrition over the long human lifespan.^{14,15}

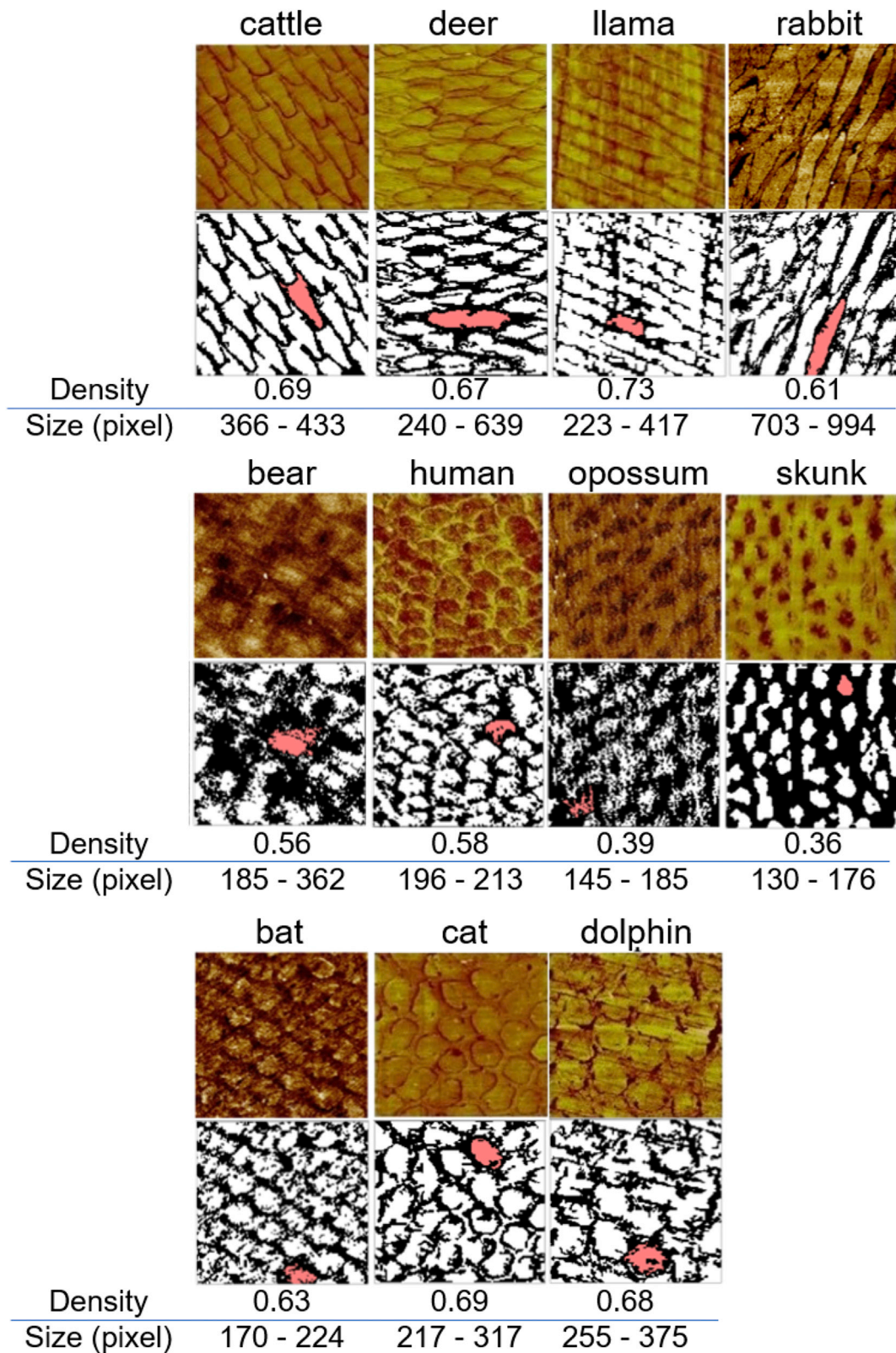


Figure 5. The enamel prism structure in various species of different feeding habits

The corresponding density, size, and morphology of enamel prisms in various species are stratified by their feeding habits. The prism structure of herbivores presents an ellipse or long strip shape, while that of omnivores resembles a circular arc or an ellipse. The carnivores are also round in shape.

DISCUSSION

In this study, we were able to show not only that there is significant variation in surface enamel hardness among mammals with different feeding behavior but also that variation in the nano-mechanical gradient of enamel in mammal species is related to their different diets. Interestingly, we were also able to demonstrate with *in situ* SR-FTIR analyses that these differences are related to their biochemical composition. The evolution of enamel structure and thickness in mammals with differing feeding strategies and longevities has resulted in differences in their nano-mechanical gradients and these evolutionary changes have played a critical role in developing differing strategies for preventing crack penetration and migration, as well as the effective promotion of energy dissipation. Understanding the structural-functional association of complex biomaterials like enamel and its relationship to other biomaterials like dentine could provide essential insights into the design of advanced materials. It would also be beneficial in various dental clinical treatments, including the development of materials for dental implants.

Limitations of the study

The limitation of this study centers around the available sample size, in particular the number of species that could be analyzed to represent each group of diet habits. Similar limitations are related to the spatial and spectral resolution that SR-FTIR analysis could be achieved. Tribological measurements could only be performed by sampling several testing spots in the sagittal section of the enamel sample after fine polishing; the data were then submitted for statistical analysis.

STAR★METHODS

Detailed methods are provided in the online version of this paper and include the following:

- KEY RESOURCES TABLE
- RESOURCE AVAILABILITY
 - Lead contact
 - Materials availability
 - Data and code availability
- EXPERIMENTAL MODEL AND SUBJECT DETAILS
 - Animals
- METHOD DETAILS
 - Sample preparation
 - Morphology and topography characterizations
 - Depth-sensing nanoindentation testing
 - SR-FTIR microspectroscopy
- QUANTIFICATION AND STATISTICAL ANALYSIS

SUPPLEMENTAL INFORMATION

Supplemental information can be found online at <https://doi.org/10.1016/j.isci.2022.105679>.

ACKNOWLEDGMENTS

We thank the colleagues and technical services provided by the “National Synchrotron Radiation Research Center,” a national user facility supported by the National Science and Technology Council, Taiwan. We thank Prof. Sheng-Hsiang Lin for providing statistical consulting services from the Biostatistics Consulting Center, National Cheng Kung University Hospital. The Center of Applied Nanomedicine, the Medical Device Innovation Center (MDIC), and the Intelligent Manufacturing Research Center (IMRC), National Cheng Kung University, supported this work from the Featured Areas Research Center Program, the Higher Education Sprout Project of the Taiwan Ministry of Education (MOE). And the authors acknowledge the grants from the National Science and Technology Council of Taiwan (MOST 104-2221-E-194-002-MY3, 108-2314-B-006-009-MY3, MOST 108-2221-E-006-228-MY3, 108-2221-E-006-228-MY3, 109-2923-E-006-005-MY3, 110-2124-M-006-005, and 110-2314-B-006-117-MY3). Professor Yeau-Ren Jeng would like to acknowledge

AC2T research GmbH (AC2T) in Austria (COMET InTribology, FFG-No.872176). Prof. Shieh would like to acknowledge Taipei Zoo for providing precious tooth samples for analysis.

AUTHOR CONTRIBUTIONS

Conceptualization: D.-B.S. and Y.-R.J.; mechanical data acquisition: J.-K.C.; FTIR spectral data acquisition and analysis: C.-T.C., Y.-N.W., and Y.-C.L.; data analysis and interpretation: C.-T.C., P.-W.W., Y.-N.W., J.-K.C., D.-B.S., Y.-R.J., and R.R.R.; first draft of the paper: C.-T.C., P.-W.W., D.-B.S., Y.-C.L.Y., Y.-R.J., and R.R.R.; review and editing: all authors. D.-B.S. and Y.-R.J. have equal contributions to conceptualization and supervision, and R.R.R. is responsible for overall guidance and final editing.

DECLARATION OF INTERESTS

The authors declare no competing interests.

Received: May 3, 2022

Revised: September 28, 2022

Accepted: November 22, 2022

Published: December 27, 2022

REFERENCES

- Yeom, B., Sain, T., Lacevic, N., Bukharina, D., Cha, S.H., Waas, A.M., Arruda, E.M., and Kotov, N.A. (2017). Abiotic tooth enamel. *Nature* 543, 95–98. <https://doi.org/10.1038/nature21410>.
- Line, S.R.P., and Novaes, P.D. (2017). The development and evolution of mammalian enamel: structural and functional aspects. *J. Morphol. Sci.* 22, 0.
- Park, S., Wang, D.H., Zhang, D., Romberg, E., and Arola, D. (2008). Mechanical properties of human enamel as a function of age and location in the tooth. *J. Mater. Sci. Mater. Med.* 19, 2317–2324. <https://doi.org/10.1007/s10856-007-3340-y>.
- Rybczynski, N., and Reisz, R.R. (2001). Earliest evidence for efficient oral processing in a terrestrial herbivore. *Nature* 411, 684–687. <https://doi.org/10.1038/35079567>.
- Qu, Q., Zhu, M., and Wang, W. (2013). Scales and dermal skeletal histology of an early bony fish *Psarolepis romeri* and their bearing on the evolution of rhombic scales and hard tissues. *PLoS One* 8, e61485. <https://doi.org/10.1371/journal.pone.0061485>.
- Zhu, M., Yu, X., and Janvier, P. (1999). A primitive fossil fish sheds light on the origin of bony fishes. *Nature* 397, 607–610. <https://doi.org/10.1038/17594>.
- Neumann, H.H. (1951). Evolution and the teeth; effects of diminishing function on the dental structure and on caries susceptibility. *N. Y. State Dent. J.* 17, 207–211.
- Zhu, M., and Yu, X. (2002). A primitive fish close to the common ancestor of tetrapods and lungfish. *Nature* 418, 767–770. <https://doi.org/10.1038/nature00871>.
- Ishiyama, M., and Teraki, Y. (1990). The fine structure and formation of hypermineralized petrodentine in the tooth plate of extant lungfish (*Lepidosiren paradoxa* and *Protopterus* sp.). *Arch. Histol. Cytol.* 53, 307–321. <https://doi.org/10.1679/aohc.53.307>.
- Marshall, G.W., Jr., Balooch, M., Gallagher, R.R., Gansky, S.A., and Marshall, S.J. (2001). Mechanical properties of the dentinoenamel junction: AFM studies of nanohardness, elastic modulus, and fracture. *J. Biomed. Mater. Res.* 54, 87–95. [https://doi.org/10.1002/1097-4636\(200101\).1002/1097-4636\(200101\)](https://doi.org/10.1002/1097-4636(200101).1002/1097-4636(200101)).
- Bruet, B.J.F., Song, J., Boyce, M.C., and Ortiz, C. (2008). Materials design principles of ancient fish armour. *Nat. Mater.* 7, 748–756. <https://doi.org/10.1038/nmat2231>.
- Jeng, Y.R., Lin, T.T., Hsu, H.M., Chang, H.J., and Shieh, D.B. (2011). Human enamel rod presents anisotropic nanotribological properties. *J. Mech. Behav. Biomed. Mater.* 4, 515–522. <https://doi.org/10.1016/j.jmbbm.2010.12.002>.
- Jeng, Y.R., Lin, T.T., and Shieh, D.B. (2009). Nanotribological characterization of tooth enamel rod affected by surface treatment. *J. Biomech.* 42, 2249–2254. <https://doi.org/10.1016/j.jbiomech.2009.06.057>.
- An, B., Wang, R., Arola, D., and Zhang, D. (2012). The role of property gradients on the mechanical behavior of human enamel. *J. Mech. Behav. Biomed. Mater.* 9, 63–72. <https://doi.org/10.1016/j.jmbbm.2012.01.009>.
- Barani, A., Bush, M.B., and Lawn, B.R. (2012). Effect of property gradients on enamel fracture in human molar teeth. *J. Mech. Behav. Biomed. Mater.* 15, 121–130. <https://doi.org/10.1016/j.jmbbm.2012.06.014>.
- Hwang, S.H. (2011). The evolution of dinosaur tooth enamel microstructure. *Biol. Rev. Camb. Phil. Soc.* 86, 183–216. <https://doi.org/10.1111/j.1469-185X.2010.00142.x>.
- Hwang, S.H. (2005). Phylogenetic patterns of enamel microstructure in dinosaur teeth. *J. Morphol.* 266, 208–240. <https://doi.org/10.1002/jmor.10372>.
- Christopher Dean, M. (2006). Tooth microstructure tracks the pace of human life-history evolution. *Proc. Biol. Sci.* 273, 2799–2808. <https://doi.org/10.1098/rspb.2006.3583>.
- Harding, H.P., Zhang, Y., Zeng, H., Novoa, I., Lu, P.D., Calfon, M., Sadri, N., Yun, C., Popko, B., Paules, R., et al. (2003). An integrated stress response regulates amino acid metabolism and resistance to oxidative stress. *Mol. Cell* 11, 619–633. [https://doi.org/10.1016/s1097-2765\(03\)00105-9](https://doi.org/10.1016/s1097-2765(03)00105-9).
- Chai, H., Lee, J.J.W., Constantino, P.J., Lucas, P.W., and Lawn, B.R. (2009). Remarkable resilience of teeth. *Proc. Natl. Acad. Sci. USA* 106, 7289–7293. <https://doi.org/10.1073/pnas.0902466106>.
- Thiery, G., Gillet, G., Lazzari, V., Merceron, G., and Guy, F. (2017). Was *Mesopithecus* a seed eating colobine? Assessment of cracking, grinding and shearing ability using dental topography. *J. Hum. Evol.* 112, 79–92. <https://doi.org/10.1016/j.jhevol.2017.09.002>.
- Staines, M., Robinson, W.H., and Hood, J.A.A. (1981). Spherical indentation of tooth enamel. *J. Mater. Sci.* 16, 2551–2556. <https://doi.org/10.1007/BF01113595>.
- Sire, J.Y., Davit-Béal, T., Delgado, S., and Gu, X. (2007). The origin and evolution of enamel mineralization genes. *Cells Tissues Organs* 186, 25–48. <https://doi.org/10.1159/000102679>.
- Mazumder, P., Prajapati, S., Bapat, R., and Moradian-Oldak, J. (2016). Amelogenin-ameloblastin spatial interaction around maturing enamel rods. *J. Dent. Res.* 95, 1042–1048. <https://doi.org/10.1177/0022034516645389>.

25. Ji, B., and Gao, H. (2004). Mechanical properties of nanostructure of biological materials. *J. Mech. Phys. Solid.* 52, 1963–1990. <https://doi.org/10.1016/j.jmps.2004.03.006>.
26. Devaraju, A., and Sivasamy, P. (2018). Comparative analysis of mechanical characteristics of sisal fibre composite with and without nano particles. *Mater. Today Proc.* 5, 14362–14366. <https://doi.org/10.1016/j.matpr.2018.03.020>.
27. Oliver, W.C., and Pharr, G.M. (1992). An improved technique for determining hardness and elastic modulus using load and displacement sensing indentation experiments. *J. Mater. Res.* 7, 1564–1583. <https://doi.org/10.1557/JMR.1992.1564>.
28. Jeng, Y.R., and Tan, C.M. (2004). Study of nanoindentation using FEM atomic model. *J. Tribol.* 126, 767–774. <https://doi.org/10.1115/TRIB2004-64013>.

STAR★METHODS

KEY RESOURCES TABLE

REAGENT or RESOURCE	SOURCE	IDENTIFIER
Experimental models: Organisms/strains		
Llama	Farm	N/A
Cattle	Farm	N/A
Deer	Farm	N/A
Rabbit	Farm	N/A
Opossum	Museum	N/A
Bear	Museums	N/A
Skunk	Taipei Zoo	N/A
Human	National Cheng Kung University Hospital	ER-100-265
Bat	Museum	N/A
Cat	Farm	N/A
Crocodile	Taipei Zoo	N/A
Dolphin	Taipei Zoo	N/A
Software and algorithms		
PRISM 5.0	GraphPad Software, California, United States	https://www.graphpad.com/support/prism-5-updates/
SAS 9.4 statistical software	SAS Institute Inc., Cary, NC, USA	https://support.sas.com/software/94/

RESOURCE AVAILABILITY

Lead contact

Further questions should be directed to the lead contact, Robert Reisz (robert.reisz@utoronto.ca).

Materials availability

This study did not generate new reagents.

Data and code availability

- The authors declare that the data supporting the findings of this study are available with the article and the supplementary information.
- This article does not report original codes.
- Any additional information required to reanalyze the data reported in this paper is available from the [lead contact](#) upon request.

EXPERIMENTAL MODEL AND SUBJECT DETAILS

Animals

The animal teeth for the analysis were provided by Prof. Shieh and Jeng obtained from extracted teeth of Taipei Zoo and Farm and by Prof. Robert Reisz from the Royal Ontario Museum. The animal species used in this study were listed as follows: llama, cattle, deer, rabbit, opossum, bear, skunk, bat, cat, crocodile, and dolphin. The human teeth were obtained from the extracted third molar of National Cheng Kung University Hospital under informed consent and were approved by the NCKU IRB (ER-100-265). The extracted teeth were maintained at room temperature in a desiccator until use.

METHOD DETAILS

Sample preparation

The teeth' enamel surfaces and axial sections were prepared for study through various processes. The specimens were stored at room temperature and were then prepared for analysis. First, the roots of the

teeth were cut out with an Isomet Low-Speed Saw (Buehler Ltd., USA). Next, the crowns were sectioned longitudinally into two-halves along the mid-labial surface using a high-speed air turbine handpiece and cooling. The specimens were then resin-embedded (Lang Dental, Erie, PA, USA), ground, and polished, yielding a flat enamel surface of about 3 × 3 mm. Grinding was performed by an Ecomet 3 grinder/polisher (Buehler Ltd., Lake Bluff, IL, USA) with ~240- to 4,000-grit silicon carbide discs at 50 rpm with jet water-cooling and debris removal (Buehler Met II grinding paper; Buehler) and a 0.05-mm alumina oxide suspension on a moist felt cloth at 250 rpm for 3 min. The final polishing was completed using only a felt cloth and jet water-cooling at 250 rpm for 30 min. Next, the polished specimens were cleaned ultrasonically in ddH₂O for 3 min. The specimen surfaces were then air-dried.

These teeth' surface morphology and structural topography have been analyzed by utilizing the atomic force microscopy (AFM) technique. In addition, nano-tribological characteristics and mechanical properties also were investigated through depth-sensing nanoindentation. The investigations were performed using mammalian molar teeth and that of a crocodile. Thirteen measurements were randomly selected for each measurement position of the enamel surface and axial section for every tooth sample. Furthermore, the nano-mechanical properties of the teeth samples were measured at the cross-section region from outer enamel to DEJ, the area was divided into twelve spaces, and the thirteen positions were sequentially imprinted from the outer enamel to DEJ.

Morphology and topography characterizations

The topography and the roughness of the enamel surfaces were measured using an AFM. The test piece was fixed on the micro-motion platform by vacuum suction, and the observation area was selected by a Charge-Coupled Device (CCD). AFM operated in contact mode with a scanning rate of 0.5 μm/s and 512 lines per sample over a scanning area of 30 × 30 μm. We tapped the probe to obtain the 2D plan, 3D perspective, roughness, point-to-point distance, and a height difference of the test piece surface. We then obtained the size and density of the enamel layer through image processing and precision calculation. The surface roughness was quantified in terms of the root mean square of the roughness height (S_q), the average roughness height (S_a), and the maximum peak-to-valley height (S_{max}). The images of prism in enamel taken by an AFM were processed by MATLAB Image Processing Toolbox to automatize enamel prism cross-section morphology objectively.

Depth-sensing nanoindentation testing

The nano-hardness and elastic modulus were extracted from the measured force vs. displacement curves following the Oliver and Pharr method^{27,28} and were evaluated utilizing a Nanoindenter (TribolIndenter, Hysitron, U.S.A.). Since the teeth of different species have different hardness, we set the indentation contact depth between 40 μm and 80 μm. We set the indentation probe to imprint the test surface to be tested with various forces. The indentation probe used in this experiment was Berkovich indenter (Bruker Hysitron TI premier) with diamond tips.^{12,13} The indentation probe imprinted the test surface to be tested with a small load and established the relationship between the strength and the indentation depth by depth sensing. The variation of the indentation probe displacement was divided into three phases over time, loading for 5s, holding for 5s, and unloading for 5s. The projected contact area of the indentation was calculated to obtain the elastic deformation and plastic deformation of the indentation probe, then the hardness value of the material could be derived by the formula of the nano-hardness as

$$H = \frac{P_{max}}{A_c} \quad (\text{Equation 1})$$

$$A_c = f(h_c) = C_1 h_c^2 + C_2 h_c + C_3 h_c^{\frac{1}{2}} + C_4 h_c^{\frac{1}{4}} \quad (\text{Equation 2})$$

Where P_{max} is the maximum load imposed on the surface of the specimen, A_c is the projected contact area between the indenter and the specimen, h_c is the contact depth, and C_1, C_2, C_3, C_4 are the constants. A calibration process of an indentation probe determines the area function. The area function uses constant C_i ($i=1,2,3,4$) to relate the indentation depth to the projected contact area A_c .

The reduced elastic modulus (E_r) of a material, as measured by indentation, was determined from the slope of the initial unloading curve as

$$E_r = \frac{\sqrt{\pi}}{2\beta} \frac{s}{\sqrt{A_c}} \quad (\text{Equation 3})$$

Where β is the geometric factor of the indentation probe.

The elastic modulus of the specimen was then determined as

$$\frac{1}{E_r} = \left(\frac{1 - \nu_s^2}{E_s} \right)_{\text{specimen}} + \left(\frac{1 - \nu_i^2}{E_i} \right)_{\text{indenter}} \quad (\text{Equation 4})$$

Where E_s , ν_s , and E_i , ν_i are the elastic moduli and Poisson's ratios of the specimen and indenter, respectively.

SR-FTIR microspectroscopy

In this investigation, the *in situ* preserved proteins of teeth were measured directly by using SR-FTIR microspectroscopy, composed of an FTIR spectrometer (Nicolet 6700, ThermoFisher Scientific, Madison, WI, USA) and a confocal infrared microscope (Nicolet Continuum; ThermoFisher Scientific, Madison, WI, USA) at the beamline BL14A1 infrared microspectroscopy (IMS) endstation of the National Synchrotron Radiation Research Center (NSRRC). The highly collimated synchrotron infrared beam was directed into the IMS endstation and focused to a $10 \times 10 \mu\text{m}^2$ infrared spot by a $32\times$ Cassegrain objective on the resin-embedded specimens into the infrared confocal microscope. The SR-FTIR spectra were collected in the mid-infrared range of $4,000\text{--}650 \text{ cm}^{-1}$, at a spectral resolution of 4 cm^{-1} with a total of 100 scans at a confocal aperture of $10 \times 10 \mu\text{m}^2$, with a lateral mapping step size of $20 \mu\text{m}$. In addition, dry nitrogen evaporated from liquid nitrogen was continuously purged into the optical path of the IMS endstation of BL14A1 to replace most of the carbon dioxide and water vapor in the optical path.

QUANTIFICATION AND STATISTICAL ANALYSIS

Kruskal-Wallis analysis was applied to test the differences in the nano-mechanical and nano-tribological properties of the enamels among the three groups of different dietary habits (Figures 1B and 1D). The Wilcoxon rank sum test was used to conduct a post-hoc test between groups (Figure 1B). The significance level was designated upon $p < 0.05$. The PRISM 5.0 (GraphPad Software, California, United States) and SAS 9.4 statistical software (SAS Institute Inc., Cary, NC, USA) were used for statistical analysis in this study.